CARBON 76 (2014) 105–112

Available at www.sciencedirect.com

ScienceDirect

journal homepage: www.elsevier.com/locate/carbon

Self-assembled folding of a biaxially compressed film on a compliant substrate

Sk. Faruque Ahmed [a,b], So Nagashima [a], Ji Yeong Lee [a], Kwang-Ryeol Lee [a], Kyung-Suk Kim [c], Myoung-Woon Moon [a,*]

[a] Institute for Multi-disciplinary Convergence of Matter, Korea Institute of Science and Technology, Seoul 130-650, Republic of Korea
[b] Department of Physics, Aliah University, DD – 45, Sector – I, Salt Lake, Kolkata 700064, India
[c] Engineering Division, Brown University, Providence, RI 02912, USA

ARTICLE INFO

Article history:
Received 22 January 2014
Accepted 15 April 2014
Available online 24 April 2014

ABSTRACT

Amorphous carbon films grown by ion beam deposition from hydrocarbon precursors on compliant polymer substrates are shown here to undergo spontaneous self-assembled folding during growth. When deposited up to 30 min, the deposition-induced stretch strain of an amorphous carbon film on poly(dimethylsiloxane) (PDMS) with a Young's modulus of 1–2 MPa reached more than 50%, which is much higher than usually observed compressive mismatch strains of approximately 1–2% on silicon. During deposition of the carbon film, compliant PDMS substrates allowed large amplitude film buckling to let in lateral growth of the film with the significant compressive mismatch strain. The film wrinkled at a low strain of approximately 1% at an early stage of deposition. Then, the wrinkled film was observed to transform its configuration through two different nonlinear modes; formations of ridges and asymmetric localized folds. Due to the biaxial nature of the deposited thin film, the wrinkled film showed herringbone or labyrinth patterns for strains less than 10%, while the folds were made in random orientations to create asymmetric disordered tessellation for strains more than 30%.

1. Introduction

Surface instabilities like wrinkling, crumpling or folding have recently been investigated in many areas of research such as biology, physics and mechanics of soft matters, and more recently, electronics with flexible substrates [1–5]. Regarding such instabilities, residually compressed thin films on thick hard substrates may delaminate and buckle as the strain energy of the film exceeds the interfacial fracture toughness [6]; in contrast, hard films on soft or compliant substrates under compressive strain have shown wrinkled or folded patterns caused by attached buckling of the films [7–9]. These corrugated surface patterns have been created by applying equi-biaxial stresses, e.g. thermal stresses, to pre-deposited thin films or ion-beam irradiated polymer skin layers [9,10]. Typical instability-induced surface patterns include two-dimensional morphologies of square, hexagonal (or triangular), kagome, herringbone or labyrinth wrinkle patterns in a single or multiple scale(s), depending on biaxiality and level of the mismatch strain between the film and the substrate. Such corrugated configurations have been reported to play an important role in the blood vessels, lungs and brains of humans [11,12]. In several artificial systems, folding was observed under a high compressive strain of shrinking

* *Corresponding author:* Fax: +82 2 958 5451.
E-mail address: mwmoon@kist.re.kr (M.-W. Moon).
http://dx.doi.org/10.1016/j.carbon.2014.04.056
0008-6223/

more than one-third the original length. Recent reports have indicated that the wrinkle patterns of stiffer layers on compliant substrates can be adopted for bio-cell motion guidance templates, nano-channels for protein condensation or optical grating devices [13–16].

The linear stability of wrinkling of a compressed thin film on a compliant substrate has been extensively analyzed to obtain the critical compressive strain and the wavelength of the wrinkle bifurcation [17–20]. Further studies on post-bifurcation behavior of wrinkles have revealed that the amplitude growth of the wrinkle leads to period or frequency multiplications followed by wrinkle localizations. The wrinkle localizations often form ridges, i.e. localized bulge of the film, or crease-like folds, i.e. inter-touches of neighboring film bulges, depending on the pre-stretch and the biaxiality of compression. For example, uniaxial plane strain compression of a stiff film on a soft substrate often folds after period quadrupling when the strain exceeds approximately 30% [20]. Such uniaxial folding is sensitive to the boundary conditions of far-field compression as well as asymmetries in the microstructure of the film and non linear deformation characteristics of the substrate [20–23]. While much of analysis has been focused on uniaxial folding, some fold patterns in natural systems, such as sulcus in the brain, are formed with nearly equi-biaxial strain conditions. Regarding formation of surface patterns under biaxial compression, analysis has been so far limited to small amplitude patterns, not large amplitude patterns created by folding [24].

Here, we firstly report the evolution of the two-dimensional self-assembled folding of a thin hard carbon film deposited on a non-prestretched compliant polymer, caused by deposition-induced mismatch strain of the film with respect to the substrate. The strain was induced by lateral growth of a diamond-like carbon (DLC) film during deposition of amorphous carbon on a poly(dimethylsiloxane) (PDMS) substrate using an ion beam bombardment method. When a thin film with a residual growth strain is deposited on a compliant substrate, as shown in the schematic in Fig. 1a, the film is susceptible to wrinkling, particularly pronounced for a large difference between the elastic moduli of the film and substrate (Fig. 1b). During the continuous deposition process of the thin film, the amplitude of the wrinkle abnormally increased as shown in Fig. 1c and d. The configuration of the film is similar to a crumpled sheet reported in the literature [25–27]. For further deposition over 30 min, a post-buckling configuration of folding in film appeared in Fig. 1c. Unlike a thin film deposited on a hard substrate, lateral growth of the deposited thin film is endorsed by the high compliance of the substrate, allowing highly curved growth configuration of the film with insignificant increase in substrate strain energy.

An amorphous carbon film was deposited on PDMS with an acetylene (C_2H_2) precursor gas using an ion beam system.

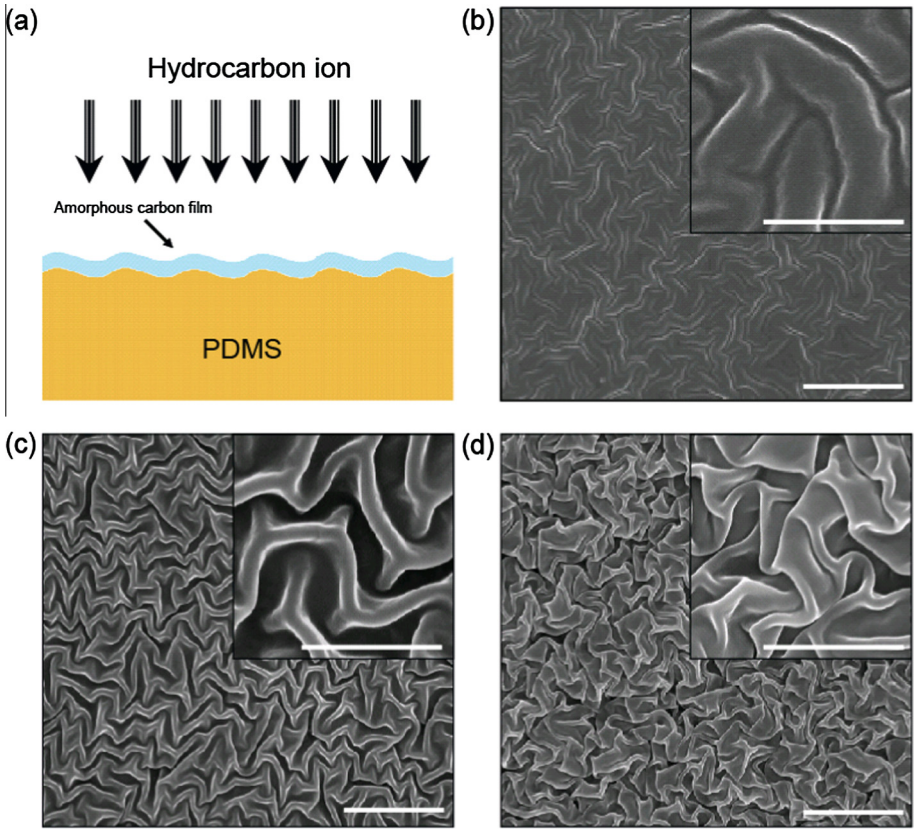

Fig. 1 – (a) A schematic of amorphous carbon deposition on PDMS; SEM micrographs of the wrinkle patterns on PDMS substrates with different amorphous carbon deposition times, (b) 30 s, (c) 5 min, and (d) 30 min. Scale bars are 3 μm (1 μm for insets). (A colour version of this figure can be viewed online.)

If deposited on hard substrates (i.e., silicon or glass) the amorphous carbon films would be typically subjected to high residual compression (1–4 GPa) and have high elastic modulus (100–300 GPa), causing the films to be susceptible to buckle delamination. The compressive strain would be relatively small, i.e., 1–2% [6,28,29]; however, if deposited on a compliant substrate wrinkles would form in the hard film [30–34]. We explored the morphological evolution of the surface configuration of amorphous carbon films deposited onto nominally flat compliant polymer substrates by varying the deposition duration, the deposition ion energy and curing composition of the substrate. We also conducted an assessment of the associated mechanics for nonlinear configurations of wrinkling and folding in films. Our chemical analysis shows that the density of the deposited amorphous carbon films on a compliant substrate is different from those on a hard substrate. The basic mechanism of thin film growth on a compliant substrate will be discussed in comparison with that on a rigid substrate. This work also discusses the potential mechanisms of nonlinear folding pattern formation in this system.

2. Experimental details

Amorphous carbon films were prepared on PDMS and Si(100) substrates using a hybrid ion beam deposition technique. PDMS substrates were prepared from a mixture of elastomer and cross-linker at a mass ratio of 10:1 (Sylgard-184, Dow Corning, MI, USA). The mixture was placed in a vacuum chamber to remove trapped air bubbles and then cured at 80 °C for 2 h, resulting in a cross-linked PDMS network. The network was cut into pieces with dimensions of 20 mm × 20 mm × 3 mm for the experiments. Amorphous carbon films were deposited in an end-hall type ion gun (DC 3 kV/6 kW, EN Technologies) [29,35]. The sample pieces were placed in the ion beam chamber, and the chamber was evacuated to a base pressure of 2×10^{-5} mbar. The distance between the ion source and the substrate holder was approximately 15 cm. Acetylene gas was introduced into the end-hall type ion gun to obtain a hydrocarbon ion with a flow rate of 8 standard cubic centimeters per minute (sccm). The anode voltage was kept at a constant value of 520 volts with a current density of 30 μA/cm^2. Radio frequency (r.f.) bias voltage was applied to the substrate holder at a bias voltage of −200 V. The amorphous carbon films were deposited by varying the deposition time from 15 s to 30 min, which resulted in amorphous carbon films with thicknesses of 1–30 nm as determined from cross-sectional images measured by a focused ion beam (FIB, Nova 600, FEI) and a high resolution transmission electron microscope (HRTEM). The surface morphologies of the deposited films with various thicknesses were measured with a scanning electron microscope (SEM, NanoSEM, FEI Company). The Young's moduli of the amorphous carbon films were calculated using the simple theory for wrinkled thin films on PDMS substrates. Raman spectroscopy analyses were performed on the deformed amorphous carbon surfaces to investigate the ion-induced structural changes in chemical bonds. The Raman measurements were made in a back-scattering geometry with a Raman spectrometer (LabRAM HR, HORIBA Jobin–Yvon Inc.) filled with a liquid-nitrogen-cooled charge-coupled device detector. The spectra were collected for 120 s under ambient conditions using a 514.5 nm argon-ion laser with a power of 0.5 mW.

3. Results and discussion

The morphology of an amorphous carbon film depended on the deposition duration. Deposition duration was varied from 30 s to 30 min, as shown in Fig. 1b–d. Under nearly equi-biaxial stress conditions, the configuration of the wrinkle in the film was close to a herringbone shape for the short duration of 30 s, as shown in Fig. 1b. As we increased the deposition or equivalently the mismatch strain, a highly irregular labyrinth type pattern was observed to have an average wavelength of 120 nm, as shown in Fig. 1c. At a longer duration of 30 min, a highly disordered tessellation configuration was observed, as shown in Fig. 1d, where the morphology is similar to that of a free crumpled sheet without any support [25,26]. As the deposition duration increased from 30 s to 5 min in Fig. 2a, the thickness of the deposited film was changed from a few nm to 10 nm. After a 5-min deposition, the

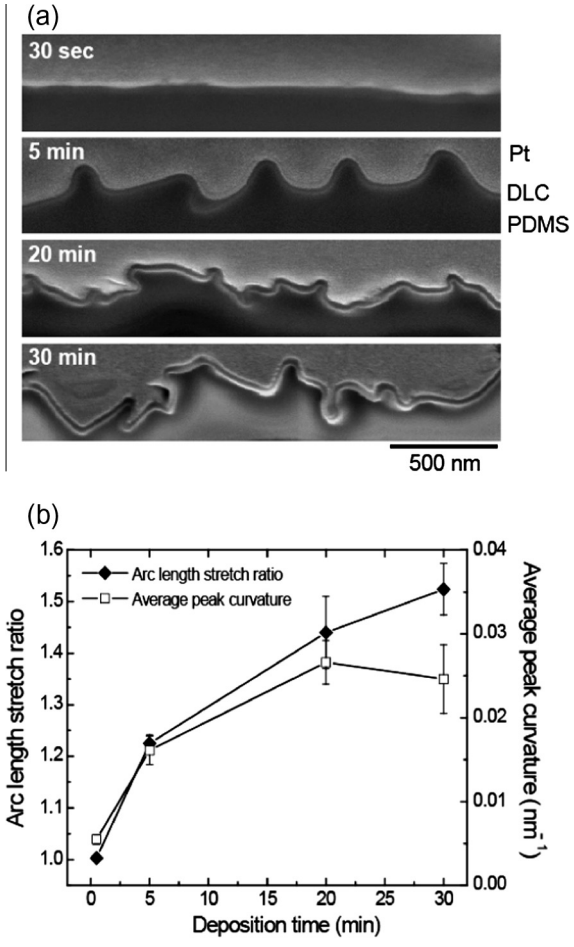

Fig. 2 – (a) FIB cross-sectional image of an amorphous carbon film on PDMS with different deposition times, and (b) variation of the arc length stretch ratio and average peak curvature of the nonlinear wrinkle with amorphous carbon deposition time.

growth rate along the thickness direction yielded substantially. After a 20-min deposition, a large deformation of the thin film was observed with a highly nonlinear folding configuration. Fold configuration was examined by cross-sectional profiles, and changes in the configuration were further enhanced as we increased the deposition duration. Interestingly, relatively symmetric ridge-mode wrinkles, termed in [36], were observed after 5 min of deposition, and then transformed into asymmetric folds after 20 and 30 min deposition durations. Unlike crease-like folds of uniaxially compressed films reported in the literature [20,25–27], the asymmetric ridge folding configuration may be induced by the equi-biaxial nature of the stress conditions in this system. This behavior is similar to the morphological transition from a checkerboard or linear-shaped wrinkle to a herringbone-shaped wrinkle as the stress level increases under equi-biaxial stress conditions [8,17]. In Fig. 2b, the relative arc length of the folded film to the original length of the flat configuration was estimated by direct measurement of the arc length (L) on the cross sectional image of the film, made by FIB sectioning. With L_0 as the horizontal distance between the ends of the trace, the nominal stretch strain was taken as $(L - L_0)/L_0$. The stretch strain of the amorphous film was measured as 50% for a 30-min deposition, which is much larger than 1–2% observed in the amorphous carbon films deposited on stiff substrates such as Si [6,28,29]. Note that the average curvature at the peak of individual patterns also increased and saturated at 0.025 nm^{-1}.

Fig. 3a shows the Raman spectra of the amorphous carbon films deposited on PDMS and Si with different deposition durations. The Raman spectra of the deposited carbon films were deconvoluted using a Gaussian distribution. The spectra possess a linear background from two peaks located at 1365 and 1540 cm^{-1} that represent disordered graphite clusters with short-range crystallinity (denoted as the D peak) and graphite-like sp^2 bonded carbon (denoted as the G peak), respectively [37]. In the Raman spectra, the G peak position shifted from 1535 to 1545 cm^{-1} as we increased the deposition duration, indicating increasing sp^2 bonded aromatic sites in the samples. The increase in crystallinity is also observed in the shape of the spectra because the intensity of the D peak increases and the shoulder is more pronounced because the G peak position is located at 1545 cm^{-1}. With increasing deposition duration, the ratio of the intensity for the D peak to the G peak (I_D/I_G) clearly increases as shown in Fig. 3b. This result suggests that as the number and/or size of the sp^2 graphite clusters increase, the amorphous carbon films become more graphitic. The stress in the amorphous carbon film is known to decrease while the sp^2 content increases. Thus, when increasing the deposition duration, the sp^2 fraction increases and the stress in the amorphous carbon film decreases [38]. The hardness of the films is associated with the full width at half maximum (FWHM) of the G peak. With decreasing FWHM of the G peak, the hardness of the amorphous carbon films decreases [39]. From the values of FWHM, we conclude that amorphous carbon films become softer with increasing deposition duration.

Fig. 3c shows the HRTEM image of a cross sectional view of the amorphous carbon film sandwiched between PDMS and platinum deposited for 20 min. From the HRTEM image, the thickness of the deposited carbon layer is clearly ~30 nm.

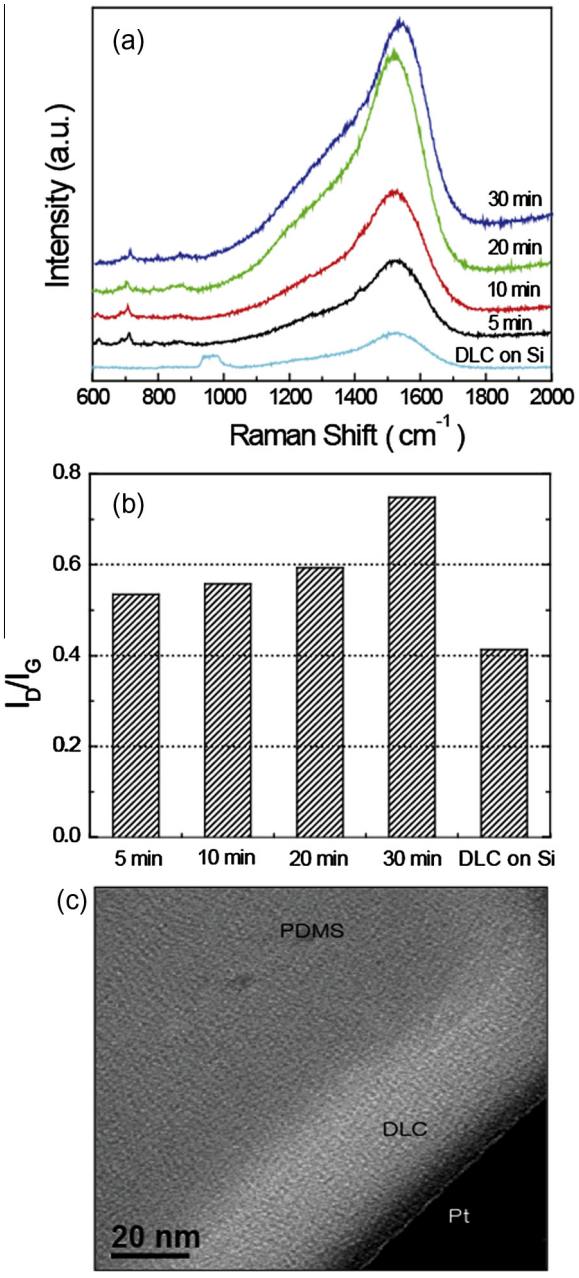

Fig. 3 – (a) Raman spectra of amorphous carbon films deposited on PDMS and Si substrates with different times, (b) corresponding ratio of the D peak to G peak (I_D/I_G), and (c) HRTEM microstructure of amorphous carbon on PDMS. (A colour version of this figure can be viewed online.)

We confirmed that the layer is amorphous in nature from the diffraction pattern (not shown here). We also observed intermixing between the amorphous carbon film and PDMS, which was presumed by the unclear interface between the two materials. However, the deposited amorphous carbon layer is brighter than the PDMS matrix because the amorphous carbon is more electron transparent than PDMS, which is composed of C, Si, and O.

It can be considered that several factors such as substrate compliance or ion beam energy or power may govern the folding behavior of the deposited thin film. First of all, to

check the compliance effect on the wrinkle or fold behavior of the deposited thin film, the compliance of PDMS was varied by changing the mixing ratio of elastomer over curing agent; 3:1, 10:1 and 20:1. It has been reported that the higher content of elastomer in mixing ratio makes PDMS softer [10,40]. It was shown that the folding on the PDMS with a lower mixing ratio, or a higher substrate stiffness, appeared to have smaller (although weakly varying) average amplitude and the characteristic wavelength than those for higher mixing ratio in Fig. 4a. The result implies that the softer PDMS may easily release the compressive strain with a larger amplitude of folding. The effect of ion beam energy was also observed on fold pattern formation in the deposited film as shown in Fig. 4b. As increased the ion beam anode voltage from 520, 750 and to 1000 V at the deposition duration of 5 min of amorphous carbon film, the average wavelength of the fold pattern also increased from 148, 265, and to 347 nm, respectively, implying that the higher the ion energy, the thicker or harder the film is deposited. The formation behavior of wrinkle pattern by ion beam deposition can be also compared with that by other methods such as plasma-enhanced chemical vapor deposition (PECVD) [41]. In previous amorphous carbon deposition by PECVD, only wrinkles, not folds, were developed although the patterns were irregular. However, if the amorphous carbon were deposited under higher energy in PECVD, fold-like pattern would be developed in the film deposited on a compliant substrate.

Chen and Hutchinson have dealt with the wrinkle types of externally compressed thin film under a biaxial stress state [8]. The wrinkle wavelength can be determined by the combination of the film thickness (h_f) and the ratio of Young's moduli between the film (E_f) and the substrate (E_s). By considering the wrinkling geometries under plane strain conditions on an infinitely deep substrate, the early stage wrinkling configuration can be assumed as $w = w_{max}\sin(\pi x/\lambda)$, and a critical strain for the onset of film wrinkling would be expressed by $e_c = 1/4 \cdot (3\overline{E}_{sub}/\overline{E}_f)^{2/3}$, where $\overline{E} = E/(1-\nu^2)$ and ν is the Poisson's ratio is the poission. Above the critical strain (e_c) for the amorphous carbon film, the wavelength (λ) for wrinkling would be predicted as

$$\lambda/h_f = \alpha \cdot \sqrt[3]{\overline{E}_f/\overline{E}_{sub}}, \quad (1)$$

where α is approximately 4.36 for the plane strain condition [17,19]. Note that the wavelength λ would increase with the increasing thickness (h_f) of the film. The wavelength varied from 100 to 250 nm when the deposition time was changed from 15 s to 5 min. After 5 min of deposition, the wrinkle pattern becomes non-sinusoidal. To estimate Young's modulus of the amorphous carbon film, Eq. (1) can be rewritten as

$$\overline{E}_f = \overline{E}_{sub} \cdot (\lambda/(\alpha h_f))^3, \quad (2)$$

where the wrinkle wavelength (λ) and the thickness of the film were measured from the experiment and the Young's modulus for the substrate was predetermined from the literature [10,40].Thus, the Young's modulus for the thin film could be estimated directly using Eq. (2). The wrinkling wavelength of the amorphous carbon film on PDMS induced by a mismatch strain was measured. Young's modulus for the PDMS substrate is approximately 2.0 MPa [10,40], and Poisson's ratio 0.5. Based on the assumption of a hyper-elastic material, Young's moduli of the amorphous carbon films were estimated with respect to the film thickness using Eq. (2). The calculated elastic moduli for the amorphous carbon films with a thickness of 1 nm turned out to be 50 GPa, which is

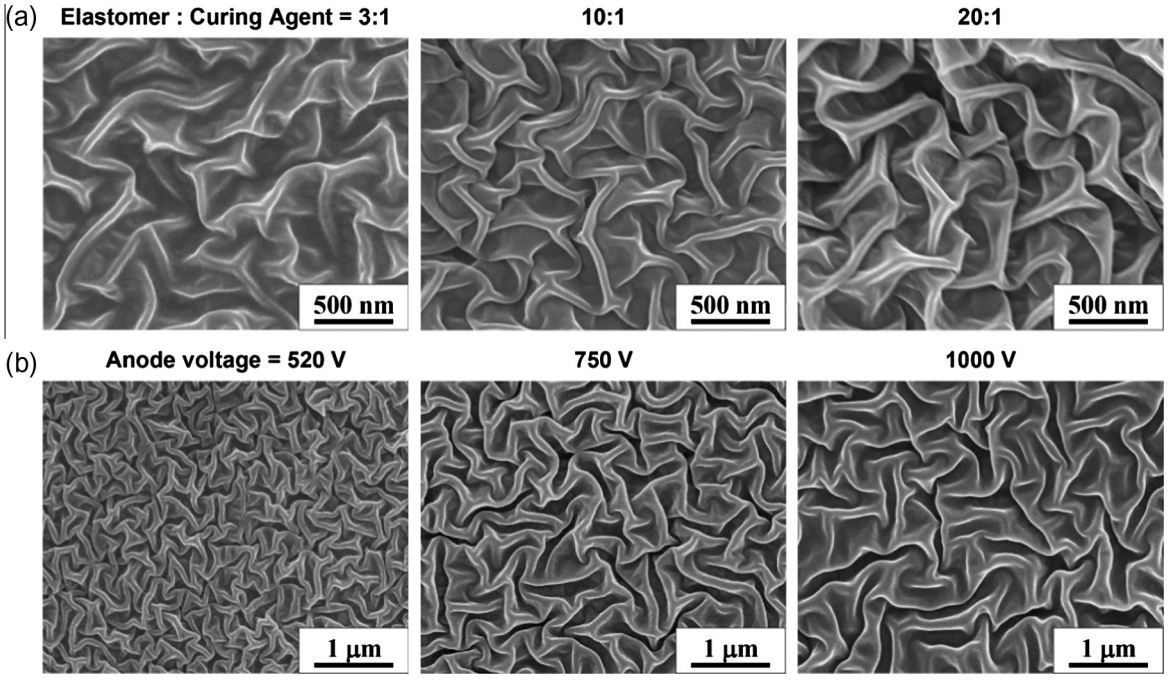

Fig. 4 – SEM images showing fold in the 5 min-deposited compressive film for (a) 3 different mixing ratios for PDMS at the fixed ion beam voltage of 520 V and substrate bias voltage of −200 V and (b) different ion beam voltages at the fixed substrate bias voltage of −200 V.

relatively more compliant than the reported value of a DLC film deposited on Si [42,43].

An increased duration of film deposition during continuous ion bombardment obviously causes an increase in the compressive strain, which is far more than the critical value for onset of wrinkling. The mechanism leading to the evolution of a very high mismatch strain over 30% can be attributed to the hyper-elastic nature of the PDMS substrates supporting the film. When ion-beam deposited on a stiff substrate, high-energy hydrocarbon ions penetrate the surface and enter subsurface interstitial sites among pre-deposited atoms, inducing structural distortion of the existing carbon network laterally constrained by the stiff substrate. This process generally causes densification of the film and an increase in the internal stress of the amorphous film [44]. For a film deposited on a stiff substrate such as silicon or glass, the film stress increases with increasing film thickness. The film eventually delaminates because the strain energy exceeds the interfacial separation energy on the stiff substrate [6,28,45]. When the film is attached to a compliant substrate, the film stress will increase at the early stage of deposition on a flat surface of the substrate as if it were deposited on a rigid substrate. However, the film will be buckled once the stress or the mismatch strain in the film exceeds the critical value of wrinkling. Once the film is wrinkled, the film stress may not increase significantly because the stress is relaxed by relatively easy stretching of the film on the compliant substrate. Subsequent deposition on a wrinkled film allows lateral growth of the film as illustrated in Fig. 5 and resulting in an in significant change in the film stress with substantial increase in the mismatch strain. Then, the longer duration of amorphous carbon film deposition brought about a further increase in the mismatch strain, as shown in Fig. 2. Upon further increase in the mismatch strain, inhomogeneous fluctuation in growth of the wrinkle amplitudes, under an effective biaxial pre-stretch made by the film deposition, will lead to growth of localized bulges, i.e. ridges, in the cost of relaxing nearby high frequency wrinkles. These localizations of bulg-

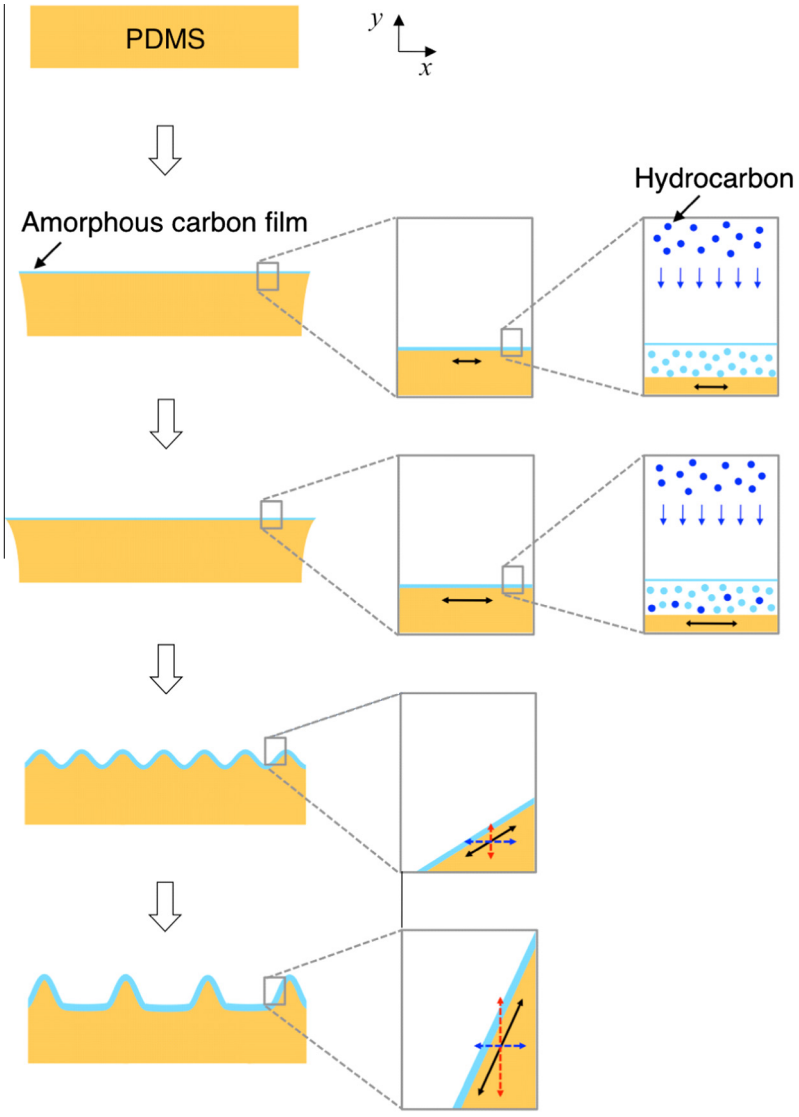

Fig. 5 – A schematic of the strain and morphological evolution during ion beam deposition. Arrows indicate a relative compressive strain in the film.

ing follow period doubling and/or quadrupling of high frequency wrinkles. In addition, the period doubling and the quadrupling often undergo irreversible bifurcation processes known as snap buckling. Such irreversible processes generally cause loss of regularization power in forming self-assembled periodic structures, producing slightly non-periodic patterns of ridges followed by asymmetric disordered tessellation of ridge folds.

Regarding the effects of the substrate pre-stretch on ridge formation, recently, the ridge mode in wrinkle configurations was calculated for a film bonded to a pre-stretched neo-Hookean substrate [22]. As the pre-stretching strain of the substrate is dominant in forming the ridge mode, a sufficiently large pre-stretch for the substrate induces ridging of the wrinkled layer [36]. This ridge mode in wrinkle evolution might be similar to the ridge shown in the cross-sectional image for a 5-min deposition in Fig. 2a. Unlike a usual sinusoidal configuration, the ridge of each wrinkle increases its height more steeply with respect to the mismatch strain. As the mismatch strain increased, the curvature of the ridge crest initially increased but quickly approached to a threshold value as shown in Fig. 2b. Due to the relaxation of accumulated strain energy along a random direction of the surface, the ridge folding became an asymmetric disordered tessellation.

4. Conclusions

Folding of a thin hard film deposited on a compliant polymer was investigated as the mismatch strain increased up to 50% in the amorphous carbon film. During deposition of amorphous carbon by ion bombardment with high energy, compliant PDMS substrates allowed lateral growth of the film, resulting in an insignificant film stress and a large increase in the mismatch strain of the film. We observed that the film wrinkled at a low strain of approximately 1% for a strong mismatch in elastic moduli between the amorphous film and compliant polymer. As the deposition duration increased, the configuration of the wrinkled film was observed to transform into two different nonlinear modes, i.e. semi-periodically distributed ridges and asymmetric localized folds, which have been generally known to form at very high compressive strains, more than 30%, in the film. Due to the biaxial nature of the mismatch strain in the deposited thin film, the wrinkled film showed herringbone or labyrinth patterns for a low mismatch strain less than 10%, while the ridge folding appeared in a pattern of asymmetric disordered tessellation for a high mismatch strain more than 30%. The newly discovered biaxial ridge-folding structures in amorphous carbon films deposited on a PDMS substrate by an ion beam deposition technique are believed to be useful for developing new (hierarchical) surface patterns of various coatings including anti-fouling marine coatings [46], low friction and anti-adhesion coatings on soft material surfaces, coatings for bio-cell motion guidance templates and coatings for nano and micro fluidic channels.

Acknowledgements

This work was financially supported in part by TES Co. Ltd. under the “Advanced Manufacturing Technology Research Center” Program of the MKE of Korea (K.R.L.) and in part by a Grant from the Global Excellent Technology Innovation R&D Program MKE (M.W.M.) and a KIST – Brown collaboration project.

REFERENCES

[1] Genzer J, Groenewold J. Soft matter with hard skin: from skin wrinkles to templating and material characterization. Soft Matter 2006;2:310–23.
[2] Mei Y, Kiravittaya S, Harazim S, Schmidt OG. Principles and applications of micro and nano scale wrinkles. Mater Sci Eng, R 2010;70:209–24.
[3] Lacour SP, Wagner S, Huang Z, Suo Z. Stretchable gold conductors on elastomeric substrates. Appl Phys Lett 2003;82:2404–6.
[4] Wang JY, Teraji T, Ito T. Fabrication of wrinkled carbon nanofilms with excellent field emission characteristics. Diam Relat Mater 2005;14:2074–7.
[5] Bowden N, Huck WTS, Paul KE, Whitesides GM. The controlled formation of ordered, sinusoidal structures by plasma oxidation of an elastomeric polymer. Appl Phys Lett 1999;75:2557–9.
[6] Moon MW, Chung JW, Lee KR, Oh KH, Wang R, Evans AG. An experimental study of the influence of imperfections on the buckling of compressed thin films. Acta Mater 2002;50:1219–27.
[7] Huang ZY, Hong W, Suo Z. Nonlinear analyses of wrinkles in a film bonded to a compliant substrate. J Mech Phys Solids 2005;53:2101–18.
[8] Chen X, Hutchinson JW. Herringbone buckling patterns of compressed thin films on compliant substrates. J Appl Mech 2004;71:597–603.
[9] Huang R. Kinetic wrinkling of an elastic film on a viscoelastic substrate. J Mech Phys Solids 2005;53:63–89.
[10] Moon MW, Lee SH, Sun JY, Oh KH, Vaziri A, Hutchinson JW. Controlled formation of nanoscale wrinkling patterns on polymers using focused ion beam. Scripta Mater 2007;57:747–50.
[11] MacLaurin J, Chapman J, Jones GW, Roose T. The study of asymptotically fine wrinkling in nonlinear elasticity using a boundary layer analysis. J Mech Phys Solids 2013;61:1691–711.
[12] MacLaurin J, Chapman J, Jones GW, Roose T. The buckling of capillaries in solid tumours. Proc R Soc A 2012;468:4123–45.
[13] Huck WTS. Artificial skins, hierarchical wrinkling. Nat Mater 2005;4:271–2.
[14] Cai DK, Neyer A, Kuckuk R, Heise HM. Optical absorption in transparent PDMS materials applied for multimode waveguides fabrication. Opt Mater 2008;30:1157–61.
[15] Harrison C, Stafford CM, Zhang W, Karim A. Sinusoidal phase grating created by a tunably buckled surface. Appl Phys Lett 2004;85:4016–8.
[16] Chung S, Lee JH, Moon MW, Han J, Kamm RD. Non-lithographic wrinkle nanochannels for protein preconcentration. Adv Mater 2008;20:3011–6.
[17] Chen X, Hutchinson JW. A family of herringbone patterns in thin films. Scripta Mater 2004;50:797–801.
[18] Cerda E, Mahadevan L. Geometry and physics of wrinkling. Phys Rev Lett 2003;90:074302.
[19] Bowden N, Brittain S, Evans AG, Hutchinson JW, Whitesides GM. Spontaneous formation of ordered structures in thin films of metals supported on an elastomeric polymer. Nature 1998;393:146–9.

[20] Sun JY, Xia S, Moon MW, Oh KH, Kim KS. Folding wrinkles of a thin stiff layer on a soft substrate. Proc R Soc A 2012;468:932–53.
[21] Brau F, Vandeparre H, Sabbah A, Poulard C, Boudaoud A, Damman P. Multiple-length-scale elastic instability mimics parametric resonance of nonlinear oscillators. Nat Phys 2011;7:56–60.
[22] Cao Y, Hutchinson JW. Wrinkling phenomena in Neo-Hookean film/substrate bilayers. J Appl Mech 2012;79:031019.
[23] Brau F, Damman P, Diamant H, Witten TA. Wrinkle to fold transition: influence of the substrate response. Soft Matter 2013;9:8177–86.
[24] Kim P, Abkarian M, Stone HA. Hierarchical folding of elastic membranes under biaxial compressive stress. Nat Mater 2011;10:952–7.
[25] Blair DL, Kudrolli A. Geometry of crumpled paper. Phys Rev Lett 2005;94:166107.
[26] Vliegenthart GA, Gompper G. Forced crumpling of self-avoiding elastic sheets. Nat Mater 2006;5:216–21.
[27] Savin T, Kurpios NA, Shyer AE, Florescu P, Liang H, Mahadevan L, et al. On the growth and form of the gut. Nature 2011;476:57–62.
[28] Moon MW, Lee KR, Oh KH, Hutchinson JW. Buckle delamination on patterned substrates. Acta Mater 2004;52:3151–9.
[29] Roy RK, Ahmed SF, Yi JW, Moon MW, Lee KR, Jun Y. Improvement of adhesion of DLC coating on nitinol substrate by hybrid ion beam deposition technique. Vacuum 2009;83:1179–83.
[30] Ahmed SF, Rho GH, Lee KR, Vaziri A, Moon MW. High aspect ratio wrinkles on a soft polymer. Soft Matter 2010;6:5709–14.
[31] Rahmawan Y, Jang KJ, Moon MW, Lee KR, Kim KS, Suh KY. Wrinkled, dual-scale structures of diamond-like carbon (DLC) for superhydrophobicity. Langmuir 2010;26:484–91.
[32] Kim SJ, Moon MW, Lee KR. Frictional behavior on wrinkle pattern of diamond-like carbon film on soft polymer. Diam Relat Mater 2012;23:61–5.
[33] Joe M, Moon MW, Oh J, Lee KH, Lee KR. Molecular dynamics simulation study on rough amorphous carbon growth by grazing incidence of energetic carbon atoms. Carbon 2012;50:404–10.
[34] Li B, Cao YP, Feng XQ, Gao H. Mechanics of morphological instabilities and surface wrinkling in soft materials: a review. Soft Matter 2012;8:5728–45.
[35] Ahmed SF, Yi JW, Moon MW, Jang YJ, Park BH, Lee SH, et al. The morphology and mechanical properties of PC/ABS modified by Ar ion beam irradiation. Plasma Proc Polym 2009;6:860–5.
[36] Zang J, Zhao X, Cao Y, Hutchinson JW. Localized ridge wrinkling of stiff films on compliant substrates. J Mech Phys Solids 2012;60:1265–79.
[37] Ferrari AC, Robertson J. Raman spectroscopy of amorphous, nanostructured, diamond-like carbon, and nanodiamond. Philos Trans R Soc London, A 2004;362:2477–512.
[38] Choi HW, Choi JH, Lee KR, Ahn JP, Oh KH. Structure and mechanical properties of Ag-incorporated DLC films prepared by a hybrid ion beam deposition system. Thin Solid Films 2007;516:248–51.
[39] Tamor MA, Vassell WC. Raman "fingerprinting" of amorphous carbon films. J Appl Phys 1994;76:3823–30.
[40] Moon MW, Lee SH, Sun JY, Oh KH, Vaziri A, Hutchinson JW. Wrinkled hard skins on polymers created by focused ion beam. Proc Natl Acad Sci USA 2007;104:1130–3.
[41] Kim SJ, Yoon JI, Moon MW, Lee KR. Frictional behavior on wrinkle patterns of diamond-like carbon films on soft polymer. Diam Relat Mater 2012;23:61–5.
[42] Lemoine P, Quinn JP, Maguire PD, Zhao JF, McLaughlin JA. Intrinsic mechanical properties of ultra-thin amorphous carbon layers. Appl Surf Sci 2007;253:6165–75.
[43] Ferrari AC, Robertson J, Pastorelip R, Beghi MG, Bottani CE. Elastic constant of diamond like carbon films by surface brillouin scattering. Mater Res Soc Symp Proc 2000;593:311–6.
[44] Robertson J. Diamond-like amorphous carbon. Mater Sci Eng, R 2002;37:129–281.
[45] Moon MW, Jensen HM, Hutchinson JW, Oh KH, Evans AG. The characterization of telephone cord buckling of compressed thin films on substrates. J Mech Phys Solids 2002;50:2355–77.
[46] Efimenko K, Finlay J, Callow ME, Callow JA, Genzer J. Development and testing of hierarchically wrinkled coatings for marine antifouling. ACS Appl Mater Interfaces 2009;1:1031–40.